Engineering Multiferroism in $CaMnO_3$

Satadeep Bhattacharjee, Eric Bousquet, and Philippe Ghosez
Physique Théorique des Matériaux, Université de Liège (B5), B-4000 Sart Tilman, Belgium

(Received 13 November 2008; published 18 March 2009)

Structural instabilities of $CaMnO_3$ are investigated from first principles. We point out that, on top of a strong antiferrodistortive instability responsible for its orthorhombic ground state, the cubic perovskite structure of $CaMnO_3$ also exhibits a weak ferroelectric instability. Although ferroelectricity is suppressed by antiferrodistortive motions, we show that it can be favored using strain or chemical engineering in order to make $CaMnO_3$ multiferroic. We finally highlight that the ferroelectric instability of $CaMnO_3$ is Mn-dominated. This illustrates that, contrary to common belief, ferroelectricity and magnetism are not necessarily exclusive but can be driven by the same cation.

DOI: 10.1103/PhysRevLett.102.117602 PACS numbers: 77.80.−e, 71.15.Mb, 75.40.Mg, 75.47.Lx

The family of ABO_3 perovskite oxide compounds constitutes an important class of multifunctional materials which, within the same simple cubic structure, exhibit a wide variety of behaviors and range from ferroelectric, piezoelectric, or nonpolar antiferrodistorted insulators to metals or superconductors, eventually combining an additional magnetic order [1]. Recently, the search for magnetoelectric multiferroics operating at room temperature has motivated the study of oxides combining ferroelectric and magnetic orders such as $BiFeO_3$ or $YMnO_3$ [2,3]. In this framework, the case of $CaMnO_3$, a magnetic insulator which remains paraelectric, was considered as a prototypical example to reveal the antagonist role of partial d-shell occupancy in respectively yielding magnetism but penalizing ferroelectricity [4].

$CaMnO_3$ is a G-type antiferromagnetic insulator [5]. It crystallizes at low temperature in a paraelectric *Pnma* orthorhombic ground-state structure which can be viewed as a small distortion of the cubic perovskite structure, produced by the tilting of oxygen octahedra [6]. Because of the Mn^{4+} configuration, $CaMnO_3$ does not exhibit Jahn-Teller distortion: In the cubic structure, the $5d$ orbitals of a Mn ion split into threefold-degenerated t_{2g} levels and twofold-degenerated e_g levels with occupation being t_{2g}^3 and e_g^0 [7]. $CaMnO_3$ does not exhibit ferroelectric distortion either. In ABO_3 compounds, ferroelectricity is usually related to the $O2p$–Bd hybridization [8], and Filippetti and Hill [4] argued that, because of the partial d-shell occupancy of Mn in $CaMnO_3$, the Mn ion is unable to accept a transfer of charge from the neighboring oxygen so that there is a strong resistance of the filled d shells with spherical symmetry to move off-center. The fact that ferroelectricity requires d^0-ness while magnetism requires partial d-state occupancy is often evoked to explain the scarcity of compounds combining both properties [2–4,9]. It also suggests that the search for multiferroic ABO_3 perovskites should be oriented toward materials in which magnetism and ferroelectricity are driven independently by the A and B cations [3,10].

Khomskii [11] further argued that since the Mn ion is in the Mn^{4+} state, the empty e_g orbitals could nevertheless take part in the charge transfer process. However, they suggested that the exactly half-filled t_{2g} orbitals might restrict the bonding between empty e_g orbitals and oxygen p orbitals by imposing Hund's rule on the e_g states. More recently, a first-principles study of the orthorhombic phase of $CaMnO_3$ [12] revealed that the static dielectric constant in that phase is very large and comparable to that of isostructural $CaTiO_3$ [13]. Since the latter is an incipient ferroelectric and its large dielectric response is coming from the softening of the highly polar ferroelectric mode, this is questioning the similar tendency of $CaMnO_3$ to exhibit ferroelectricity.

In this Letter, we first carefully reinvestigate from first principles the structural instabilities of cubic $CaMnO_3$. We point out that, contrary to common belief, $CaMnO_3$ does develop a weak ferroelectric (FE) instability at its equilibrium volume. However, like in $CaTiO_3$, the latter is hidden by a much deeper antiferrodistortive (AFD) instability which is responsible for the orthorhombic ground state. FE and AFD instabilities are, however, in competition in $CaMnO_3$, and we then explore the possibility of making it multiferroic using either strain or chemical engineering.

Our calculations were done in the framework of density functional theory using the ABINIT package [14]. In all of our calculations, we imposed a G-type antiferromagnetic order. We worked within the generalized gradient approximation (GGA), using the recent Wu-Cohen functional [15], which is known to be very accurate in predicting the volume of solids. This choice is particularly important here since ferroelectricity is strongly sensitive to the volume. We used optimized pseudopotentials [16] generated with OPIUM [17], treating as valence states the $3s$, $3p$, $3d$, and $4s$ states of Mn, the $3s$, $3p$, and $4s$ states of Ca, and the $2s$ and $2p$ states of O. The wave function was expanded in plane waves, up to a kinetic energy cutoff of 55 Ha. Integrals over the Brillouin zone were replaced by sums on a $6 \times 6 \times 6$ mesh of special k points.

First, we reinvestigated the structural, electronic, and dielectric properties of $CaMnO_3$ in the cubic perovskite structure. In this high-symmetry phase, the atomic positions are fixed by symmetry so that the only structural degree of freedom is the lattice constant. Our calculations provide a relaxed value $a_0 = 3.74$ Å in excellent agreement with the experimental estimate of 3.73 Å [18]. Within the GGA, this relaxed structure is correctly predicted to be insulating. Although significantly smaller than the experimental value (3.1 eV [19]) because of the well-known density functional theory band gap problem, our calculated band gap of 0.54 eV agrees with previous local density approximation (LDA) calculations [4,20].

On top of calculations at the optimized lattice parameter, we also considered structures at $a_{-2\%} = 0.98$, $a_0 = 3.67$ Å and $a_{+2\%} = 1.02$, $a_0 = 3.81$ Å. The results are summarized in Table I. We observe that the electronic band gap decreases when increasing the volume, which is expected from the evolution of the crystal field in a compound where the gap arises from the splitting between t_{2g} and e_g orbitals. $CaMnO_3$ nevertheless remains an insulator at the three volumes, even at the GGA level.

The Born effective charges (Z^*) and optical dielectric constants (ϵ_∞) are also reported in Table I and compare well with previous calculations [4,20]. We notice that the Born effective charges present features very similar to those of ferroelectric perovskites [21], with Z^*_{Mn} and $Z^*_{\mathrm{O}\|}$ (for O displacement parallel to the Mn-O bond) being *anomalously* large. In prototypical ferroelectric perovskites such as $BaTiO_3$, these anomalous Z^* were shown to be a key feature to produce a giant destabilizing dipolar interaction at the origin of the ferroelectric instability [22]. Although the dielectric constant is larger in $CaMnO_3$ as properly noticed in Ref. [4] and will so better screen the Coulomb interaction, it remains surprising that $CaMnO_3$ does not exhibit any tendency to ferroelectricity in spite of its giant Z^*.

We therefore computed the phonon frequencies within the cubic perovskite structure in order to identify the structural instabilities inherent to $CaMnO_3$. At the optimized volume, we surprisingly identified a small FE instability related to an unstable polar mode with an imaginary frequency $\omega_{\mathrm{FE}} = 13i$ cm^{-1}. However, we also observed, within the same structure, a much larger AFD instability associated to a nonpolar oxygen rotational mode with an imaginary frequency $\omega_{\mathrm{AFD}} = 213i$ cm^{-1}. It is, in fact, the condensation of this latter mode with different amplitudes along the different directions that generates the observed orthorhombic ground state [12]. The case of $CaMnO_3$ is therefore very similar to that of $SrTiO_3$ or $CaTiO_3$: It develops both FE and AFD instabilities, and the absence of a ferroelectric ground state is not directly related to its magnetic character but to a much larger tendency to oxygen rotations. Both types of instability are in competition, and we explicitly checked that, once the dominant AFD distortion is condensed, the small FE instability is suppressed by anharmonic effects.

Performing a similar characterization at different volumes, we observe in Fig. 1 that the AFD instability is rather independent of the lattice constant. At the opposite, the FE instability is strongly sensitive to volume, a result totally similar to what was previously reported for titanates [1]. This might explain why no FE instability was previously reported from LDA calculations which typically underestimate the volume by 1%–2%.

Following the original idea of Cochran [23], the ferroelectric instability in perovskite oxides is usually explained in terms of a close competition between short-range (SR) forces, which tend to favor the high-symmetry phase, and long-range (LR) Coulomb interactions, which tend to destabilize the structure. In order to clarify whether this idea still applies to $CaMnO_3$, we decomposed the full dynami-

TABLE I. Lattice constant, energy gap, Born effective charges, and optical dielectric constant of cubic $CaMnO_3$ at three different volumes. $O_\perp$ and $O_\|$ refer, respectively, to O displacements parallel and perpendicular to the Mn-O bond.

	a_{cell} (Å)	E_g (eV)	Z^*_{Ca} ($\|e\|$)	Z^*_{Mn} ($\|e\|$)	$Z^*_{\mathrm{O}_\perp}$ ($\|e\|$)	$Z^*_{\mathrm{O}_\|}$ ($\|e\|$)	ϵ^∞
$a_{-2\%}$	3.67	0.64	2.63	7.75	−1.79	−6.80	10.42
a_0	3.74	0.54	2.61	8.16	−1.80	−7.18	11.49
$a_{+2\%}$	3.81	0.41	2.60	8.68	−1.82	−7.64	13.24

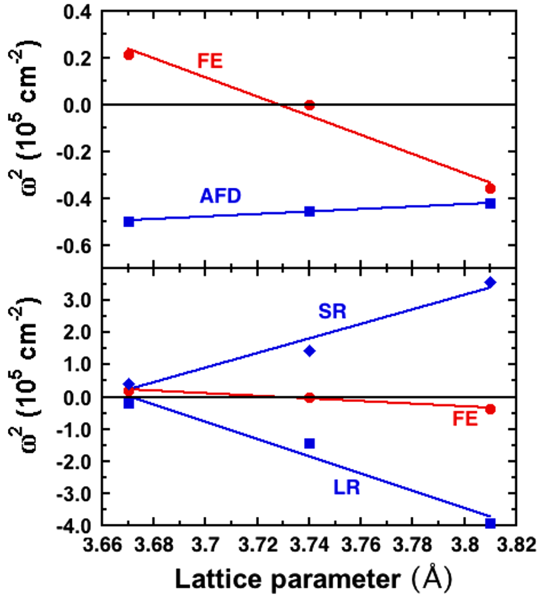

FIG. 1 (color online). Top: Evolution with the lattice constant of the square of the frequency of FE mode (red circles) and AFD mode (blue squares) of cubic $CaMnO_3$. Bottom: Decomposition of the square of the FE frequency (red circles) into its short-range (blue diamonds) and long-range contributions (blue squares) as explained in the text.

cal matrix ($\tilde{D}_{\text{tot}}$) into a model LR electrostatic dipole-dipole part ($\tilde{D}_{\text{LR}}$) and a remaining SR part ($\tilde{D}_{\text{SR}}$) [22]. This allows us to quantify the respective LR and SR contributions to the unstable FE frequency as

$$\underbrace{\langle \eta_{\text{FE}} | \tilde{D}_{\text{tot}} | \eta_{\text{FE}} \rangle}_{\omega^2_{\text{FE}}} = \underbrace{\langle \eta_{\text{FE}} | \tilde{D}_{\text{LR}} | \eta_{\text{FE}} \rangle}_{\omega^2_{\text{LR}}} + \underbrace{\langle \eta_{\text{FE}} | \tilde{D}_{\text{SR}} | \eta_{\text{FE}} \rangle}_{\omega^2_{\text{SR}}},$$

where η_{FE} is the FE mode dynamical matrix eigenvector. The results are summarized in Fig. 2 and are comparable to those previously reported for BaTiO_3 [22]: The small FE instability is a consequence of a delicate balance between SR and LR forces and arises from a giant negative LR contribution directly related to the anomalously large Z^* values. We explicitly checked that, considering them at their own optimized volume, CaMnO_3 develops a LR contribution ($\omega_{\text{LR}} = 378.4i\ \text{cm}^{-1}$) even larger than CaTiO_3 ($\omega_{\text{LR}} = 345i\ \text{cm}^{-1}$), in spite of its larger dielectric constant. The smaller FE instability of CaMnO_3 is related to stronger SR forces associated to its smaller equilibrium volume ($\omega_{\text{SR}} = 378.2\ \text{cm}^{-1}$ in CaMnO_3 versus $\omega_{\text{SR}} = 313\ \text{cm}^{-1}$ in CaTiO_3).

The natural tendency of CaMnO_3 to develop a ferroelectric distortion being established, it might now be asked which cation is driving the FE instability. To clarify this issue, the involvement of each type of atom within the FE mode dynamical matrix eigenvector η_{FE} is reported in Table II [24]. Inspection of this table points out that the progressive softening of the FE mode when increasing the volume is closely related to the concomitant increase of the Mn atom motion. This involvement of the Mn atom which has the largest Z^*, combined to a lower extent with the small increase of Z^* itself, produces a significant increase of the mode effective charge and of the related destabilizing LR interaction. This clearly establishes the Mn-driven character of the ferroelectric instability. CaMnO_3 provides therefore a first prototypical example of a magnetic perovskite $AB\text{O}_3$ compound in which ferroelectricity and magnetism are driven by the *same* cation, illustrating the fact that magnetism and ferroelectricity are not necessarily exclusive.

The absence of a FE phase transition in CaMnO_3 being related to the competition with the AFD instability, we now investigate to what extent it would be possible to favor ferroelectricity and so, eventually, make CaMnO_3 multiferroic using either strain or chemical engineering.

From Fig. 1, it appears that FE and AFD instabilities exhibit a very different sensitivity to strain, a fact that can be potentially exploited to favor the ferroelectric distortion. Since applying a negative isotropic pressure is not easily achievable in practice, we rather explore the possibility to make CaMnO_3 ferroelectric under epitaxial strain as it could be achieved in epitaxial thin films. In ferroelectric oxides, it is well known [25] that large enough compressive epitaxial strains typically favor a ferroelectric c phase (with the polarization out of plane) while tensile strains favor a ferroelectric a phase (with polarization in plane), but no systematic data are available for the impact of epitaxial strain on the AFD distortion. So we performed full structural relaxation at fixed epitaxial strains. For compressive strains, we observed that the ground state of CaMnO_3 remains AFD distorted and, unfortunately, paraelectric for strains as large as -4%, roughly the largest epitaxial strain experimentally achievable. At the opposite, for tensile strains, it appeared that a polar ground state is obtained for strains larger than about $+2\%$. Beyond this critical value, the system preserves its oxygen rotations but acquires an additional in-plane polarization estimated from a Berry phase calculation to $4\ \mu\text{C}\,\text{cm}^{-2}$ at an in-plane lattice constant of 3.82 Å. This provides a theoretical demonstration that CaMnO_3 can be made ferroelectric by strain engineering. We note that, in spite of the weak FE motion, the Mn-O-Mn angle remains close to that of the orthorhombic phase ($\approx 156°$), so that the Néel temperature should remain similar to that in bulk.

Another way to increase the volume and provide more space for the FE distortion of the Mn atom is to perform atomic substitution and to replace Ca by a larger ion. To

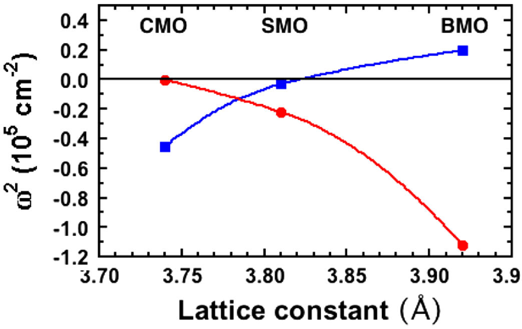

FIG. 2 (color online). Square of the frequency of FE (red circles) and AFD (blue squares) modes of CaMnO_3 (CMO, $a_0 = 3.74$ Å), SrMnO_3 (SMO, $a_0 = 3.81$ Å), and BaMnO_3 (BMO, $a_0 = 3.92$ Å) at their own equilibrium volume.

TABLE II. Lattice constant (a_{cell}), AFD (ω_{AFD}) and FE (ω_{FE}) phonon frequencies, FE mode effective charge (Z^*_{FE}), and involvement of each type of atom in the FE mode eigenvector [24] for different compounds in the cubic perovskite structure. $\text{Ca}_{0.5}\text{Ba}_{0.5}\text{MnO}_3$ results are for an ordered supercell with Ca and Ba alternating along the [111] direction.

$AB\text{O}_3$	a_{cell} (Å)	ω_{AFD} (cm^{-1})	ω_{FE} (cm^{-1})	Z^*_{FE} (e)	η^2_{A} (%)	η^2_{Mn} (%)	η^2_{O} (%)
CaMnO_3	3.67	$223i$	146	7.51	59	0	41
	3.74	$213i$	$13i$	10.22	34	5	61
	3.81	$205i$	$189i$	13.48	8	26	66
SrMnO_3	3.81	$55i$	$148i$	14.65	0	19	81
$\text{Ca}_{0.5}\text{Ba}_{0.5}\text{MnO}_3$	3.83	$150i$	$216i$	15.28	0	21	79
BaMnO_3	3.92	140	$335i$	19.24	0	22	78

support this idea, we compare in Fig. 2 and Table II the behavior of $CaMnO_3$, $SrMnO_3$, and $BaMnO_3$, each of them in the same prototypical cubic perovskite structure at their own equilibrium volume. It clearly appears that increasing the size of the A cation strongly favors the FE distortion that is the only remaining instability in $BaMnO_3$. Again, the FE instability is Mn-dominated, further illustrating that ferroelectricity and magnetism can be driven by the same cation. Going further, we see that the atomic substitution goes beyond a simple volume effect since, together with favoring ferroelectricity, bigger A cations also suppress the possibility of oxygen rotation. From that viewpoint, atomic substitution of Ca by a bigger atom appears even more promising than epitaxial strain to produce a ferroelectric ground state.

To support this idea, we considered a $Ca_{0.5}Ba_{0.5}MnO_3$ alloy. Working first within the virtual crystal approximation (VCA) [26], we obtained a relaxed lattice constant $a_0 = 3.84$ Å and observed a strong FE instability ($\omega_{\mathrm{FE}} = 224i\ \mathrm{cm}^{-1}$) while the AFD instability was totally suppressed ($\omega_{\mathrm{AFD}} = 110\ \mathrm{cm}^{-1}$). Considering then an ordered supercell in which Ca and Ba ions alternate along the [111] direction, the relaxed lattice constant ($a_0 = 3.83$ Å) and the FE instability ($\omega_{\mathrm{FE}} = 215i\ \mathrm{cm}^{-1}$) were very similar to VCA but the AFD mode was unstable ($\omega_{\mathrm{AFD}} = 150i\ \mathrm{cm}^{-1}$). This points out that the AFD mode might be very sensitive to atomic order, but both approaches predict a dominant FE instability. This confirms that, eventually combined with strain engineering, partial substitution of Ca by Ba will favor ferroelectricity and is a promising way to make $CaMnO_3$ multiferroic.

Figure 2 also suggests that the FE instability dominates the AFD in the cubic polymorph of $SrMnO_3$. This is consistent with the absence of oxygen rotations reported in Ref. [27] and certainly asks for further experimental check of a possible FE ground state. In the absence of AFD, the Mn-O-Mn angle will be close to 180° even with a FE distortion, yielding a Néel temperature significantly larger than in bulk $CaMnO_3$ and likely in the range 200–250 K [27]. In view of the large epitaxial strain (+2.5%), we also propose that $SrMnO_3$ films on [001] $SrTiO_3$ [28] should develop a significant in-plane polarization.

In conclusion, we have investigated from first principles the lattice dynamics of cubic $CaMnO_3$. We pointed out that, together with a strong AFD instability responsible for its orthorhombic ground state, $CaMnO_3$ also surprisingly exhibits a weak FE instability at its equilibrium volume. Going further, we highlighted that both strain and chemical engineering can be used to favor the FE distortion and make $CaMnO_3$ multiferroic. Finally, we also showed that the FE instability of $CaMnO_3$, $SrMnO_3$, and $BaMnO_3$ is Mn-dominated, illustrating that ferroelectricity and magnetism are not necessarily exclusive and can be driven by the same cation. All of this suggests alternative strategies in the search for multiferroic ABO_3 compounds.

This work was supported by the European projects MaCoMuFi and FAME-EMMI and by the Interuniversity Attraction Poles Program (P6/42)—Belgian State-Belgian Science Policy. Simulations were done on the supercomputer MareNostrum at the Barcelona Supercomputing Center.

[1] *Physics of Ferroelectrics: A Modern Perspective*, edited by K. M. Rabe, Ch. H. Ahn, and J.-M. Triscone, Top. Appl. Phys. Vol. 105 (Springer, Berlin, 2007).
[2] M. Fiebig, J. Phys. D **38**, R123 (2005).
[3] R. R. Ramesh and N. Spaldin, Nature Mater. **6**, 21 (2007).
[4] A. Filippetti and N. A. Hill, Phys. Rev. B **65**, 195120 (2002).
[5] S. F. Matar, Prog. Solid State Chem. **31**, 239 (2003).
[6] K. R. Poeppelmeir, M. E. Leonowicz, J. C. Scanlon, J. M. Longo, and Y. B. Yelon, J. Solid State Chem. **45**, 71 (1982).
[7] D. I. Khomskii and G. A. Sawatzky, Solid State Commun. **102**, 87 (1997).
[8] R. E. Cohen, Nature (London) **358**, 136 (1992).
[9] N. A. Hill, J. Phys. Chem. B **104**, 6694 (2000).
[10] N. A. Spaldin and M. Fiebig, Science **309**, 391 (2005).
[11] D. I. Khomskii, J. Magn. Magn. Mater. **306**, 1 (2006).
[12] S. Bhattacharjee, E. Bousquet, and Ph. Ghosez, J. Phys. Condens. Matter **20**, 255229 (2008).
[13] E. Cockayne and B. P. Burton, Phys. Rev. B **62**, 3735 (2000).
[14] X. Gonze *et al.*, Comput. Mater. Sci. **25**, 478 (2002).
[15] Z. Wu and R. E. Cohen, Phys. Rev. B **73**, 235116 (2006).
[16] A. M. Rappe, K. M. Rabe, E. Kaxiras, and J. D. Joannopoulos, Phys. Rev. B **41**, 1227 (1990).
[17] http://opium.sourceforge.net.
[18] E. O. Wollan and W. C. Koehler, Phys. Rev. **100**, 545 (1955).
[19] J. H. Jung *et al.*, Phys. Rev. B **55**, 15 489 (1997).
[20] A. Filippetti and N. A. Spaldin, Phys. Rev. B **68**, 045111 (2003).
[21] Ph. Ghosez, J.-P. Michenaud, and X. Gonze, Phys. Rev. B **58**, 6224 (1998).
[22] Ph. Ghosez, X. Gonze, and J.-P. Michenaud, Europhys. Lett. **33**, 713 (1996).
[23] W. Cochran, Adv. Phys. **9**, 387 (1960).
[24] The involvement of each type of atom in η_{FE} is quantified from individual contributions to the square of the norm: $\langle \eta_{\mathrm{FE}} \mid \eta_{\mathrm{FE}} \rangle = \eta_A^2 + \eta_{\mathrm{Mn}}^2 + \eta_{\mathrm{O}}^2 = 1$.
[25] O. Dieguez, K. M. Rabe, and D. Vanderbilt, Phys. Rev. B **72**, 144101 (2005).
[26] Ph. Ghosez, D. Desquesnes, X. Gonze, and K. M. Rabe, AIP Conf. Proc. **535**, 102 (2000).
[27] O. Chmaissem *et al.* Phys. Rev. B **64**, 134412 (2001).
[28] P. Paghan, W. Prellier, and B. Mercey, Phys. Rev. B **70**, 184419 (2004).